Journal Pre-proofs

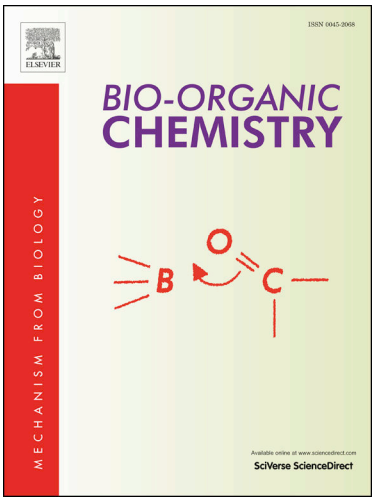

Design, Synthesis, and Evaluation of a Novel Benzamidine-Based Inhibitor of VEGF-C binding to Neuropilin-2

Ahmed M. Said, Matthew W. Parker, Craig W. Vander Kooi

PII: S0045-2068(19)31958-3
DOI: https://doi.org/10.1016/j.bioorg.2020.103856
Reference: YBIOO 103856

To appear in: *Bioorganic Chemistry*

Received Date: 15 November 2019
Revised Date: 11 March 2020
Accepted Date: 14 April 2020

Please cite this article as: A.M. Said, M.W. Parker, C.W. Vander Kooi, Design, Synthesis, and Evaluation of a Novel Benzamidine-Based Inhibitor of VEGF-C binding to Neuropilin-2, *Bioorganic Chemistry* (2020), doi: https://doi.org/10.1016/j.bioorg.2020.103856

Design, Synthesis, and Evaluation of a Novel Benzamidine-Based Inhibitor of VEGF-C binding to Neuropilin-2

Ahmed M. Said[a,c]*, Matthew W. Parker[b], Craig W. Vander Kooi[b]*

[a]Department of Chemistry, University at Buffalo, The State University of New York, Buffalo, NY, 14260, United States

[b]Department of Molecular and Cellular Biochemistry, Center for Structural Biology, University of Kentucky, Lexington, KY 40536, United States

[c]Pharmaceutical Organic Chemistry Department, Faculty of Pharmacy, Helwan University, Ein-Helwan, Helwan, Cairo 11795, Egypt

*To whom correspondence should be addressed:

Dept of Chemistry, University at Buffalo, Buffalo, NY, 14260 E-mail: ahmedmoh@buffalo.edu

Dept. of Biochemistry, University of Kentucky, Lexington, KY 40536 E-mail: craig.vanderkooi@uky.edu

Declarations of interest: none

ABBREVIATIONS

Nrp: Neuropilin; VEGF: Vascular Endothelial Growth Factor; DIEA: diisopropylethylamine, DMF: dimethylformamide; EDCI.HCl: 1-ethyl-3-(3-dimethylaminopropyl)carbodiimide hydrochloride; HOAc: acetic acid, HOAt: 1-Hydroxy-7-azabenzotriazole; HPLC: high pressure liquid chromatography; Boc-: tert-butyloxycarbonyl; MeOH: methanol; TFA: trifluoroacetic acid; GIPC: GAIP Interacting Protein, C-terminus

ABSTRACT

The Neuropilin (Nrp) family of cell surface receptors have key physiological and pathological functions. Nrp2 is of particular interest due to its involvement in tumor metastasis. Currently, peptide and small molecule inhibitors that target Nrp utilize arginine-based molecules which have limitations due to high inherent flexibility and issues related to stability. Further, there are no known small molecule inhibitors specific for Nrp2. Recent molecular insights identify a key ligand binding region in the b1 domain of Nrp2 responsible for binding the C-terminus of its cognate ligand VEGF-C. Based on this, we report the discovery of a novel benzamidine-based inhibitor that functions through competitive inhibition of VEGF-C binding to Nrp2. Further, we have explored inhibitor functionality and selectivity by defining its structure-activity relationship (SAR) providing valuable insights on this benzamidine-based family of Nrp2 inhibitors. This study provides the basis for further development of a potent and specific small molecule inhibitor that competitively targets pathological Nrp2 function.

Graphical abstract

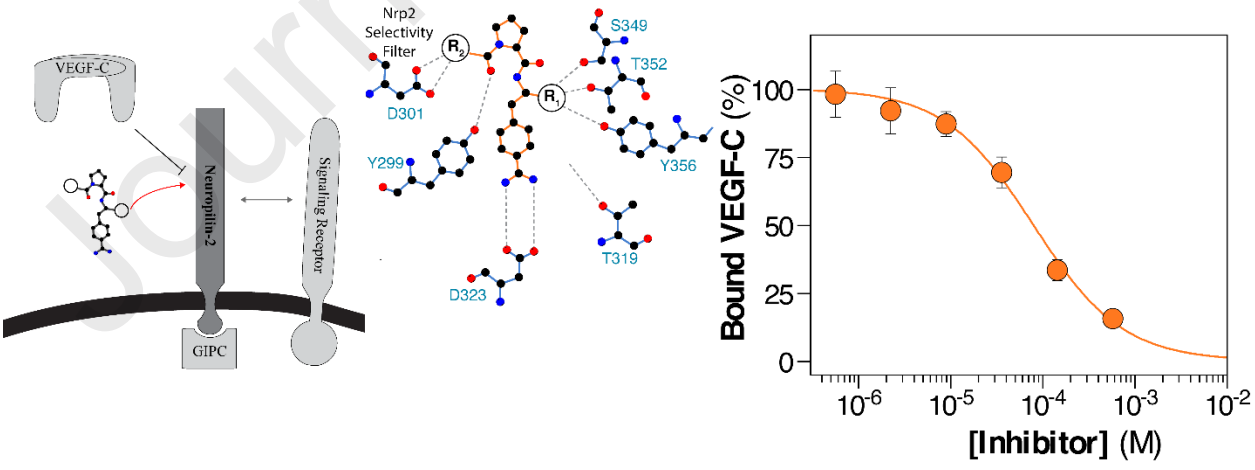

KEYWORDS: Receptor, Neuropilin, Nrp-2, VEGF, Lymphatic, Angiogenesis, Benzamidine

1. Introduction

Members of the Neuropilin (Nrp) family are multi-functional cell surface receptors [1]. There are two Nrp family members, Nrp1 and Nrp2, both of which function by integrating multiple steps of cellular activation and function by binding to extracellular, cell surface, and intracellular proteins, thus allowing it to function as a central physical nexus integrating cellular activation and directional migration [2]. The biological function of Nrp is critically connected to its function as an essential co-receptor for the Vascular Endothelial Growth Factor (VEGF) family of secreted growth factors. VEGF-dependent cellular activation occurs within the context of a ligand/receptor holocomplex that includes VEGF ligand and two cell surface receptors, Nrp and VEGFR.

There are five VEGF family members, VEGF-A, -B, -C, -D and placental (PlGF), three VEGFR family members, VEGFR-1, -2, -3, and two Nrp family members, Nrp1 and Nrp2. The different ligand and receptor combinations have specific biological functionality. VEGF-C and VEGF-D selectively control lymphangiogenesis [3]. VEGF-C functions specifically through VEGFR-2/3 [4-7] and Nrp2 [8, 9]. Endothelial cells of homozygous VEGF-C knockout mice do not sprout to form lymph vessels resulting in an alymphatic embryo and embryonic lethality [10]. Equivalently, overexpression of VEGF-C results in selective induction of lymphatic but not vascular endothelial cell proliferation and lymphatic vessel enlargement [11]. In addition to its critical physiological role, VEGF-C signaling is also important for pathological lympangiogenesis associated with both aberrant loss of function in lymphedema [12] or gain of function in tumorigenesis and metastasis [13-15]. VEGFR-2/3 have dual functionality in both angiogenesis and lymphangiogenesis [16]. In contrast, Nrp2 knockout mice display normal angiogenesis but abnormal lymphatic vessel development [17], similar to the tissue specific function observed in the VEGF-C knockout mouse [10, 17]. It is thought that under normal signaling conditions VEGF-

C simultaneously engages both VEGFR and Nrp2 [18], although it has also been demonstrated that Nrp2 can function in VEGF-C signaling independent of its role as a co-receptor with VEGFR [15].

A variety of inhibitory modalities to target the Nrp system have been explored. Peptide-based inhibitors of Nrp have been identified, but have suffered from limited stability and selectivity [19-23]. Antibody-based inhibition was reported as promising, but showed significant side effects [15]. Indeed, receptor clustering and aberrant activation of circulating cells by antibodies has been reported [24]. The development of small molecule inhibitors of Nrp is actively being pursued [21, 25]. Small molecule inhibitors are of particular interest since they are more readily amenable to iterative optimization of both binding affinity and selectivity and are often more cost effective. To date, peptide and small molecule inhibitors developed to target Nrp utililze arginine-based molecules to engage the CT-Arg ligand binding pocket. However, the use of arginine and arginine-like molecules in several scaffolds show limitations due to high inherent flexibility and issues related to stability.

Efforts to date have primarily focused on inhibiting Nrp1. However, inhibitors that specifically target Nrp2 are needed since Nrp2-dependent VEGF-C signaling is important in a variety of tumors and overexpression of these factors is correlated with advanced stage disease and poor prognosis [13, 14]. The Nrp2/VEGF-C signaling axis contributes to tumorigenesis via multiple mechanisms. Mimicking its physiological function, VEGF-C signaling via Nrp2 stimulates lymphatic vessel recruitment to tumors and directly contributes to cancer metastasis [15]. Importantly, the role of VEGF-C and Nrp2 in tumorigenesis is not exclusively associated with aberrant lymphangiogenesis. Indeed, *in situ* studies have demonstrated that autocrine VEGF-C signaling in breast cancer cells stimulates cellular motility [26]. Further, recent reports indicate

that cancer cell survival is enhanced through VEGF-C/Nrp2-dependent autophagy [27] and that autocrine Nrp2 signaling maintains the population of cancer stem cells [28]. VEGF-C also functions to protect prostate cancer cells from oxidative stress in a Nrp2-dependent fashion [29]. Thus, selective inhibition of Nrp2 represents a promising, multipronged anti-cancer therapeutic strategy.

Recent molecular insights have opened up new avenues for the development of a potent and specific Nrp2 inhibitor. The Nrp ligand binding pocket is located in the b1 coagulation factor domain and specifically binds to ligands that possess a carboxy-terminal arginine (CT-Arg) [30, 31]. Additionally, the basis for selective ligand binding by the Nrp family has been demonstrated, and involves a selectivity filter formed by interactions between the ligand and the L1 coagulation factor loop of Nrp [32, 33]. Importantly, the interaction is not a typical protein-protein interaction interface, which tend to be broad and difficult to target. Instead, Nrp2 binding utilizes a defined binding pocket with a limited number of interactions and is amenable to targeting by a small molecule inhibitor. In the current study, we identify a novel chemical scaffold for use in the development of Nrp inhibitors. We find that substituted benzamidine's are able to bind to the CT-Arg binding pocket and we define its structure-activity relationship (SAR), providing initial optimization of potency and selectivity for Nrp2.

2. Results and Discussion

2.1. Chemistry

Scheme 1: Synthesis of Inhibitor **2**:

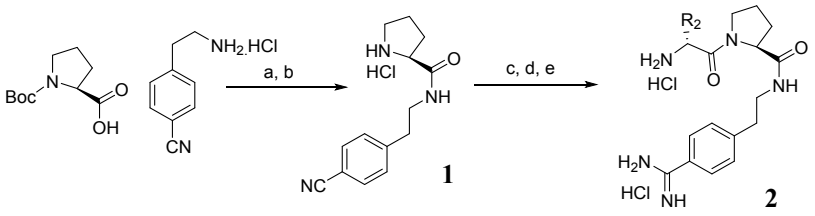

Reagents and conditions: (a) EDCI, HOAt, DIEA, DMF, 16 h; (b) 3 N methanolic HCl, 3 h at 0 °C; (c) *N-Boc*-D-Phenylalanine, EDCI, HOAT, DIEA, DMF, 16 h; (d) Hydroxylamine HCl, DIEA, anhydrous MeOH, 16 h; followed by Ac_2O, AcOH, 30 min then H_2, 10% Pd/C, 12 h; (e) 3 N methanolic HCl, 3 h at 0 °C.

The general synthesis of inhibitors (**2**) starts with an amide coupling between *N-Boc*-L-Proline and the commercially available 4-(2-Aminoethyl)benzonitrile hydrochloride using EDCI / HOAt in presence of DIEA (Scheme 1). The *Boc*- protecting group was removed with 3 N methanolic HCl to give **1** as hydrochloride salt. Intermediate **1** was reacted with *N-Boc*-D-Phenylalanine using EDCI / HOAt in presence of DIEA. The resulting amide was stirred with hydroxylamine hydrochloride and DIEA in anhydrous methanol for 16 h to form the corresponding hydroxyamidine. The hydroxyamidine were then used directly in the next step. The hydroxyamidine were stirred with acetic anhydride in acetic acid for 30-45 min. 10% Pd/C was then added and the mixture was hydrogenated. The *Boc* group was removed with 3 N methanolic HCl. The final product (**2**) was further purified using reverse-phase HPLC to a purity > 95%.

Scheme 2: Synthesis of Intermediates (**3a-3c**):

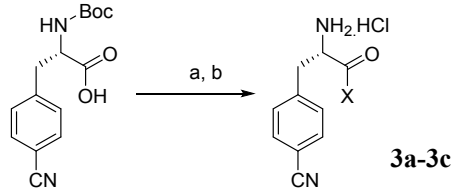

3a	X= -OBn
3b	X= -OMe
3c	X= -$NHCH_3$

Reagents and conditions: (a) K_2CO_3, X-Br, DMF, 4 h at 80 °C or in case of **3c** CH_3NH_2, EDCI, HOAt, DIEA, DMF, 16h; (b) 3 N methanolic HCl, 3 h at 0 °C.

The synthesis of intermediates (**3a-3c)** (Scheme 2) starts with an ester formation between the *N-Boc*-4-cyano-L-phenylalanine, except for intermediate **3c** an amide formation using methylamine and EDCI / HOAt in presence of DIEA was performed (Scheme 2), and the corresponding Alkyl bromide and potassium carbonate in DMF. The product formed was further stirred in 3 N methanolic HCl to remove the Boc-group to give **3a-3c** as hydrochloride salts.

Scheme 3: Synthesis of Inhibitors (**5-13**):

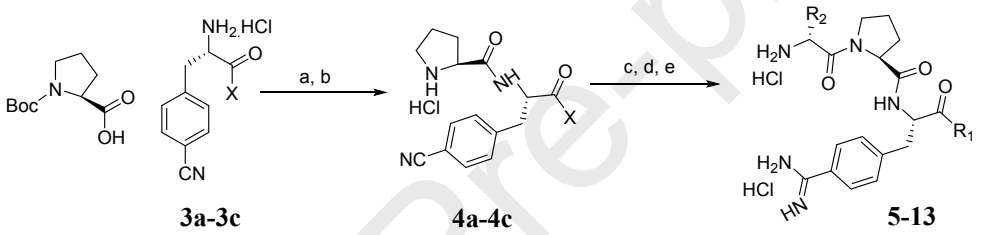

Reagents and conditions: (a) EDCI, HOAt, DIEA, DMF, 16 h; (b) 3 N methanolic HCl, 3 h at 0 °C; (c) different *N-Boc*-D-amino acids, EDCI, HOAt, DIEA, DMF, 16 h; (d) Hydroxylamine HCl, DIEA, anhydrous MeOH, 16 h; followed by Ac_2O, AcOH, 30 min then H_2, 10% Pd/C, 12 h; (e) 3 N methanolic HCl, 3 h at 0 °C.

The general synthesis of inhibitors (**5-13**) starts with an amide coupling (Scheme 3) between *N-Boc*-L-Proline and intermediates (**3a-3c**) using EDCI / HOAt in presence of DIEA (Scheme 3). The *Boc*- protecting group was then removed using 3 N methanolic HCl to give (**4a-4c**) as hydrochloride salt. Based on the final inhibitor structure, the corresponding intermediates **(4a-4c)** were reacted with different *N-Boc*-D-amino acids using EDCI / HOAt in presence of DIEA. The resulting amides were stirred with hydroxylamine hydrochloride and DIEA in anhydrous methanol for 16 h to form the corresponding hydroxyamidine. The hydroxyamidine were then used

directly in the next step. The hydroxyamidine were stirred with acetic anhydride in acetic acid for 30-45 min. 10% Pd/C was then added and the mixture was hydrogenated. The *Boc* group was removed with 3 N methanolic HCl. The final products (**5-13**) were further purified using reverse-phase HPLC to a purity > 95%.

2.2. Design of a benzamidine based Nrp2 inhibitor.

Recent structural studies have revealed the basis for the binding of VEGF-C to the Nrp2 core b1 ligand binding domain [33]. In examining the ligand binding site of Nrp2, it is notable that the side-chain of the CT-Arg not only engages in a salt bridge with D323 but is braced between Y299 from the L1 loop and Y356 from the L3 loop (Figure 1A). This led us to hypothesize that a benzamidine moiety might be utilized in place of arginine as the basis for a novel Nrp inhibitor. Indeed, bioisosteric replacement for the arginine by the more conformationally rigid benzamidine group was previously performed and is advantageous in optimization of binding mode and potency used in thrombin inhibitors [34-36]. CT-Arg is necessary but not sufficient for Nrp engagement, since additional residues N-terminal to the Arginine are required. Previous work demonstrates that Pro was the preferred amino acid in the position N-terminal to the CT-Arg in peptides that bind to Nrp [22]. Additionally, specific Nrp2/VEGF-C interactions employ direct interactions between VEGF-C and residues within the L1, L5, and L3 loops of the Nrp2 b1 domain, with D301 playing a critical role as an electrostatic selectivity filter [33]. Thus, a scheme was designed to produce dual substituted Pro-benzamidine based inhibitors (Figure 1B). This design has the benefit of being suitable for combinatorial synthesis as well as allowing flexibility in design to obtain maximum potency by varying substitution at the R1 position as well as enhancing selectivity by varying substitution at the R2 position.

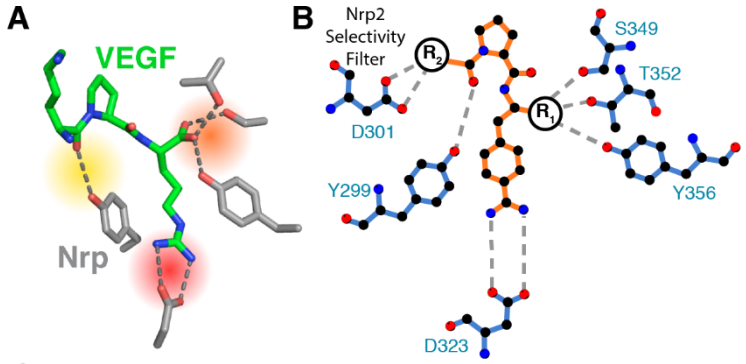

Figure 1: Design of benzamidine-based inhibitors of Nrp2. A) CT-Arg binding pocket of Nrp2 highlighting key interaction interfaces B) Model of a benzamidine based inhbitor in the VEGF-C binding pocket of Nrp2.

2.3. Testing of a benzamidine based Nrp2 inhibitor

As an initial test if a substituted benzamidine could bind to Nrp2 and inhibit VEGF-C binding, we sythensized a benzamidine-based molecule with a carboxylate in the R1 position (**5**) (Figure 2A). We utilized a competitive binding assay to assess the ability of potential inhibitors to block the binding of AP-tagged VEGF-C to plate adsorbed Nrp2. Inhibition was measured as a dose-dependent loss of retained AP activity due to competitive displacement of ligand. Strikingly, compound **5** fully competitively inhibited VEGF-C binding to Nrp2, with an IC_{50} = 78 µM (Figure 2B, Table 1).

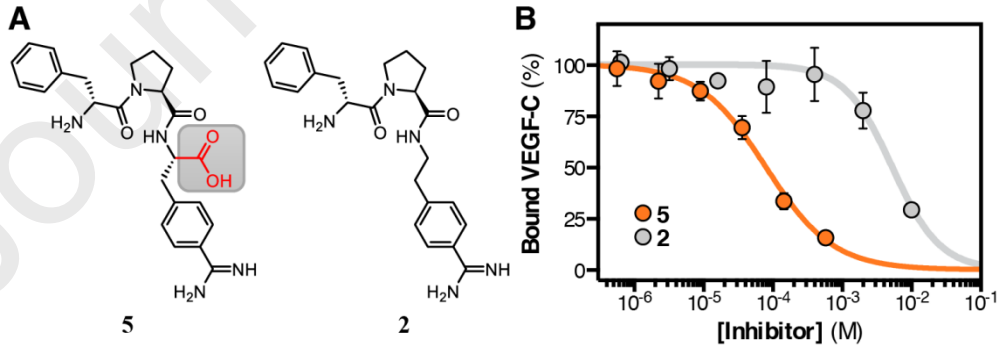

Figure 2: Discovery of benzamidine-based inhibitors of Nrp2. A) Initial lead compound with (**5**) and without (**2**) carboxylate. B) Inhibitory potency of **5** and **2** in blocking VEGF-C binding to Nrp2. Data points represent the mean value and standard deviation, N=3. Lines represent the fit used for determintation of the IC_{50}.

To confirm that this was specifically interacting with the CT-Arg binding pocket, we additionally tested the same molecule without the carboxy-group (**2**) (Figure 2A). Strikingly, we observed a 70-fold reduction in inhibition of the binding of VEGF-C to Nrp2 (IC_{50} = 5.4 mM) (Figure 2B, Table 1). These data define a novel molecular entity with unique functional groups as a lead for Nrp2 inhibition.

Table 1: Inhibitory potency of variants of the R1 and R2 positions versus Nrp2/VEGF-C

Compound	-R1	-R2	Inhibitory potency Nrp2 (IC_{50}) (Log IC_{50} ± S.E.)
5	-COOH	D-Phe	78 μM (-4.11 ± 0.04)
2	-H	D-Phe	5440 μM (-2.27 ± 0.07)
12	-COOCH3	D-Phe	201 μM (-3.70 ± 0.03)
13	-CONHCH3	D-Phe	6040 μM (-2.22 ± 0.05)
6	-COOH	4-amidine D-Phe	112 μM (-3.95 ± 0.08)
7	-COOH	D-Ser	140 μM (-3.85 ± 0.06)
8	-COOH	D-Asp	178 μM (-3.75 ± 0.06)
9	-COOH	D-HomoSer	48 μM (-4.32 ± 0.06)
10	-COOH	D-Tyr	171 μM (-3.77 ± 0.10)
11	-COOH	D-Lys	36 μM (-4.44 ± 0.10)

2.4. Inhibitor optimization

We next sought to define the SAR of (**5**) for Nrp2 binding and optimize its potency and selectivity. We first examined substitution at the carboxy postion, which is predicted to make a series of hydrogen bonds with residues from the Nrp2 L3 loop (R1, Figure 1). We tested the effect of substitution at R1 of the carboxylate of (**5**) with of an ester (**12**) or amide (**13**). Intriguingly, while an ester was accommodated with only a modest effect on potency in the R1 position, IC_{50}=201μM (**12**, Table 1), substitution with an amide was extremely deleterious IC_{50} = 6 mM (**13**,

Table 1). These data provide guidance on further inhibitor design as well as helping to explain why the vast majority of Nrp2-engaging proteins and peptides have a CT-Arg. The modest reduction in potency observed with the ester may help to explain why certain binding partners without a CT-Arg, but with highly flexible glycine following the Arg, can bind in the Nrp2 ligand binding pocket.

Because it showed maximal potency, we maintained the R1 group as a carboxylate and next sought to optimize the R2 position (Figure 1). Variation of this position was intended to allow engagement of the Nrp2 selectivity filter located in the second shell of interactions in the Nrp2 ligand binding pocket to enhance both potency and selectively [32, 37]. We replaced the Phe with amino acids that could hydrogen bond and/or were polar or charged. These replacements included aromatics 4-amidine D-Phe **(6)** and tyrosine **(10)**, neutral hydrophilics serine **(7)** and homoserine **(9)**, and charged aspartate **(8)** and lysine **(11)**. The observed potency ranged from 36-178μM (Table 1). Intriguingly, the greatest potency was observed with lysine **(11)** and homoserine **(9)**.

Table 2: Specific inhibitory potency of variants for Nrp2/VEGF-C versus Nrp1/VEGF-A

Compound	Inhibitory potency Nrp1 (IC_{50}) (Log IC_{50} ± S.E.)	Fold selectivity for Nrp2 or Nrp1
5	57 μM (-4.25 ± 0.02)	1.4
12	125 μM (-3.90 ± 0.05)	1.6
6	68 μM (-4.17 ± 0.06)	1.6
7	59 μM (-4.23 ± 0.05)	2.4
8	66 μM (-4.18 ± 0.06)	2.7
9	123 μM (-3.91 ± 0.11)	2.6
10	92 μM (-4.04 ± 0.05)	1.9
11	70 μM (-4.15 ± 0.05)	1.9

We next tested the selectivity of the most potent compounds by comparing their ability to inhibit Nrp2/VEGF-C interactions with Nrp1/VEGF-A interactions (Table 2). The majority of

previously reported peptides, such as the phage-display matured peptide ATWLPPR, show a two-fold preference for Nrp1 [38]. Similar preference for Nrp1 is observed with the majority of the benzamidine based inhibitors. Strikingly, we find that both (**9**) and (**11**) showed both improvents in potency along with correlated 2-fold preferential binding to Nrp2. This is the first report of an inhibitor that shows preference for Nrp2.

To explore the mechanism for Nrp2-selectivity, inhibitors were docked into Nrp2. Docking of (**11**), which shows the greatest potency, showed a very narrow range of conformations with the benzamidine in the CT-Arg position interacting with D323. Strikingly, the unique Lys at the R2 position forming a salt-bridge with D301 from the Nrp2 selectivity filter, providing a clear basis for the surperior potency and selectivity of (**11**) (Figure 3A, pink circle). Docking of (**9**) showed a greater range of conformations, but the majority showed CT-Arg-like engagement with the homoserine moiety at the R2 position forming a hydrogen bond with D301 (Figure 3B). This is intriguing, and also provides an explanation for the difference between (**7**) and (**9**), since (**7**) has the shorter serine at R2 and so does not have sufficient length to form this hydrogen bond. These data provide a clear basis for understanding both the observed enhanced potency and Nrp2 selectivity of this class of benzamidine-based Nrp2 inhibitors.

Further, this also provides a means to enhance the potency and selectivity of Nrp2 inhibition with further modifications. Given the reported differences in endogenous Nrp ligand [32, 37], further optimization of inhibitors to take advantage of differences in the coagulation factor loops at the tip of the b1 domains will likely results in further improvements to both binding potency and selectivity. While the selectivity filter centered on Nrp2 D301 has been discussed, there are other significant differences that could provide additional selectivity. These include variable L3 loop residues. While the core residues that that contribute to CT-Arg binding are

conserved, other residues are highly variable including in the L3 loop which in Nrp2 is 353-QNG and is Nrp1 is 350-KKK. The majority of reported Nrp1 inhibitors show modest potency (mid-μM) similar to that reported for these Nrp2-targeting benzamidine-based inhibitors. Significant potency gains for peptide-derived inhibitors of Nrp1 have been observed with other methods such as multimerization [39] and with chemical diversification [40-42], providing paths for increased potency.

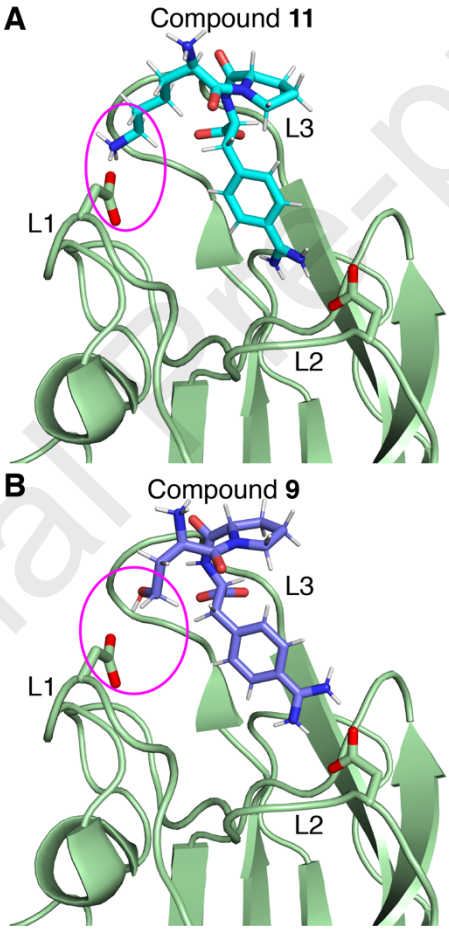

Figure 3: Docking of Nrp2 selective inhibitors. Docking of compounds A) **11** and B) **9** supports a ligand-like CT-Arg binding mode via engagement with the Nrp2 coagulation factor loops (labelled L1-L3) and a critical role for the Nrp2 L1 loop residue D301 engagement by the inhibitor R2-functionality (pink circle) in determining Nrp2 selectivitiy.

3. Conclusions

In this study, we have utilized medicinal chemistry coupled with structure-based design strategies to identify a benzamidine-based inhibitor of Nrp2. A benzamidine-based lead compound has been identified which competitively and preferentially inhibits Nrp2 ligand binding. Further development of this inhibitor to enhance potency and selectivity will open up a novel mechanism for targeting pathological Nrp2 function.

4. Materials and Methods

4.1. Biochemical methods

Competitive inhibition of Nrp ligand binding was assayed with a plate-based binding assay, as previously described [33, 43, 44]. Briefly, Nrp2-b1b2 and Nrp1-b1b2 affinity plates were produced using his-tagged bacterial expressed protein obtained from pET28b (Novagen/EMD Millipore) in Rosetta Gami-2(DE3) (Novagen/EMD Millipore, Billerica, MA) cells. Nrp protein was purified using sequential Immobilized Metal Affinity Chromatography (IMAC) (HIS-Select HF Nickel Affinity Gel, Sigma-Aldrich, St. Louis, MO) followed by heparin affinity chromatography (HiTrap Heparin HP, GE Healthcare Life Sciences, Pittsburgh, PA). Purified Nrp was diluted to 50 μg/mL with 50 mM Na_2CO_3 pH 10.4 and immediately added to 96-well protein high-bind microplates (Plate #9018, Corning, Corning, NY) and incubated for 1 h at 37°C, aspirated, washed 5x 100 μL with PBS-T (phosphate buffered saline, 0.1% Tween 20), and stored with 100 μL PBS-T at 4°C. Cognate ligands, VEGF-C for Nrp2 and VEGF-A for Nrp1, were produced as Alkaline Phosphatase (AP) fusion proteins using Chinese Hamster Ovary suspension cells (CHO-S) from the pAPtag-5 vector (GenHunter Corporation, Nashville, TN). Inhibition of Nrp-ligand binding

was measured in the presence of increasing concentrations of inhibitor. Inhibitors were pre-mixed with AP-tagged ligand, added to Nrp-affinity plates for 1 hr, washed 4x100 µL with PBS-T, incubated for 5 min, aspirated, 100 µL of 1X AP substrate added [45], and the reaction quenched with 100 µL of 0.5 M NaOH. Retained ligand was detected as a function of the evolution of para-nitrophenol, measured at 405 nm absorption on a SpectraMax M5 microplate reader (Molecular Devices, Sunnyvale, CA). The absorbance of BSA-coated control wells was used to background correct the data. Inhibition potency was determined by fitting retained ligand (AP activity) with increasing inhibitor concentration to determine the half-maximal inhibitory concentration (IC_{50}). Experiments were performed in triplicate. IC_{50} values were obtained using Prism (Graphpad Software, La Jolla, CA) with a four-parameter fit. Results are reported for each inhibitor as the mean IC_{50} ± standard error.

The initial cartoon of inhibitors in the Nrp2 ligand binding site was constructed using Ligplot+ [46]. Docking was accomplished using DockThor v2.0 (https://dockthor.lncc.br/v2/) [47]. Inhibitor structures were prepared using MarvinSketch 20.6.0 (ChemAxon ,http://www.chemaxon.com) and docked with fully enabled rotational bonds into the structure of VEGF-C bound Nrp2-b1b2 [33] (PDB ID 4QDQ) with ligand removed. Docking results were analyzed by assessing the scoring fuction of clusters for twenty four runs. Molecular graphics were generated using Pymol (www.pymol.org).

4.2. Chemistry

4.2.1. General methods

Reagents were obtained from commercial suppliers and used without further purification. Anhydrous solvents were purchased as sealed bottles from either Fisher-Acros (AcroSeal™) or Aldrich (Sure-seal™) and were maintained under an argon atmosphere. Solvent removal was

performed on a rotary evaporator equipped with a 20-60°C water bath and a self-contained aspirator. Thin-layer chromatography (TLC) was performed on Analtech (Newark, DE) 200micron Silica Gel F coated on polyethylene sheets. Visualization was accomplished with 254nm UV light or iodine staining. The silica gel used in the flash chromatography was 40-75μm flash grade purchased from Sorbent Technologies (Atlanta, GA). All amino acids used are L unless otherwise noted. Proton and carbon nuclear magnetic resonance were performed in deuterated solvents purchased from Cambridge Isotope Laboratories, Inc (Andover, MD) on the following instrument: Varian Inova 400MHz. 1H-NMR data is reported in the following format: chemical shift (ppm values in relation to TMS or appropriate solvent peak), multiplicity (s= singlet, d= doublet, t= triplet, q = quartet, dd = doublet of doublets, d of t= doublet of triplets, complex = combinations of peaks resulting from different molecular conformations, m= multiplet, br = broad peak), coupling constant(s), and integration. Low resolution ESI mass spectrometry was performed on a Thermo Finnigan LCQ Advantage instrument using 60% methanol in water with 1% acetic acid or 60% acetonitrile in water with 0.1% trifluoroacetic acid as the mobile phase. High resolution mass spectrometry both ESI and EI were performed on a Thermo Finnigan MAT 95 XL instrument. Preparative and semi-preparative HPLC instrumentation included a Milton Roy gm 4000 gradient programmer, Milton Roy Constametric I and III pumps, a Rheodyne 7125 injector with a 5.00 mL sample loop, and a Knauer Variable Wavelength Detector set at either 218 nm or 254 nm with a preparative flow cell. The HPLC columns employed included a Varian Microsorb C18, 10 μm, 100 A pore, 21 mm X 250 mm with a guard column (Preparative, Column A) used with a flow rate of 10 mL / min, a Varian Microsorb Dynamax C18, 10 μm, 100 A pore, 10 mm X 250 mm (Semi-prep, Column B) used with a flow rate of 2.5 mL / min, a Phenomenex LUNA C18(2), 5 μm, 100 A pore, 21 mm X 250 mm with Security Guard cartridge 83 (Preparative,

Column C) used with a flow rate of 10 mL / min, and a Phenomenex LUNA C18(2), 5 μm, 100 A pore, 2.1 mm X 100 mm used with a flow rate of 0.200 mL / min. Yield refers to isolated material by mass. All final compounds used to acquire biological, or crystallographic data were at least 95% pure by LC-MS analysis.

4.2.2. General procedure for amide coupling

Amine (1.00 eq), amino acid (1.10 eq), HOAt (1.10 eq) and EDCI (1.10 eq) were dissolved in anhydrous DMF. After 10 min DIEA (2.20 eq) was added. The reaction was allowed to stir for 16 h. The mixture was diluted with EtOAc. The EtOAc was washed three times with 1 N HCl, three times with saturated sodium bicarbonate, and three times with brine. The organic layer was dried with sodium sulfate, filtered through filter paper, and concentrated to give the product. The products were purified with flash chromatography whenever needed.

4.2.2. General procedure for Ester formation

N-Boc-4-cyano-L-phenylalanine (1.0 eq) was dissolved in 10 ml anhydrous DMF. The corresponding Alkyl bromide (1.2 eq) was added followed by anhydrous K_2CO_3 (2.5 eq) and the mixture was heated to 80 °C. The temperature was maintained for 4 h under argon stream. The reaction was quenched with water and the resulting suspension was extracted with 50 ml EtOAc two times. The organic fraction was washed three times with 50 ml brine, dried over anhydrous sodium sulfate, and evaporated under vacuum to give the desired product which was subjected to further step without further purification.

4.2.3. General procedure for Boc-deprotection

The Boc-protected compound was dissolved in 3 N methanolic HCl (3 ml per 1 mmol compound) at 0 °C. The solution was then stirred at room temperature for 3 h, and the solvent was removed

under vacuum to give the product. The products were purified with semi-preparative reverse phase HPLC whenever needed, or when the product is a final compound.

4.2.3. General Procedure for the Benzamidine Synthesis

The cyano containing compound (1.0 eq) and Hydroxylamine hydrochloride (5.0 eq) were dissolved in 20 mL anhydrous methanol and left for 30 min stirring then DIEA (5.0 eq) was added. The mixture was left stirring overnight and monitored by TLC. The reaction solvent was removed under vacuum and the residue was taken up in 50 mL EtOAc. The EtOAc was washed three times with 50 mL water followed by three times with 50 mL brine. The organic layer was dried over anhydrous sodium sulfate, filtered and concentrated to give the oxime. All the oximes were identified by LCMS. The oxime (1.0 eq) was dissolved in 15 mL glacial acetic acid. Acetic anhydride (1.2 eq) was added to the mixture and left to stir for 30 min then 10% Pd/C (0.05 eq) was added and the mixture was poured into the Parr bottle, which was put on to a Parr hydrogenation apparatus and the bottle was subjected to 3 charge/purge cycles with hydrogen gas. The reaction was then charged with 50-55 psi hydrogen and shaken for 12 h. The reaction solvent was filtered through celite to remove the Pd/C followed by several acetonitrile washes of the bottle and celite. The Acetonitrile fractions were combined and concentrated. The Boc- containing crude was stirred in 3 N methanolic HCl and left to stir for 3 h then the solvent was evaporated under vacuum to give the desired product. The crude products were further purified by RP-HPLC (Column A, 10% MeOH for 10 min, then a linear gradient to 100% methanol over 45-60 min) to give the hydrochloride salts as the final product.

Supplementary Data

Supplementary data includes detailed synthesis and characterization of all compounds, as well as representative NMR spectra.

Acknowledgements

We thank members of the Vander Kooi laboratory for helpful discussions and comments. In addition, we thank Prof. David Hangauer for his support. This work was supported by National Institutes of Health grant R01GM094155 (C.W.V.K.).

5. REFERENCES

[1] M.W. Parker, H.F. Guo, X. Li, A.D. Linkugel, C.W. Vander Kooi, Function of members of the neuropilin family as essential pleiotropic cell surface receptors, Biochemistry 51(47) (2012) 9437-46.
[2] H.F. Guo, C.W. Vander Kooi, Neuropilin Functions as an Essential Cell Surface Receptor, J Biol Chem 290(49) (2015) 29120-6.
[3] T. Karpanen, C.A. Heckman, S. Keskitalo, M. Jeltsch, H. Ollila, G. Neufeld, L. Tamagnone, K. Alitalo, Functional interaction of VEGF-C and VEGF-D with neuropilin receptors, FASEB J 20(9) (2006) 1462-72.
[4] E. Stuttfeld, K. Ballmer-Hofer, Structure and function of VEGF receptors, IUBMB Life 61(9) (2009) 915-22.
[5] V. Joukov, K. Pajusola, A. Kaipainen, D. Chilov, I. Lahtinen, E. Kukk, O. Saksela, N. Kalkkinen, K. Alitalo, A novel vascular endothelial growth factor, VEGF-C, is a ligand for the Flt4 (VEGFR-3) and KDR (VEGFR-2) receptor tyrosine kinases, EMBO J 15(7) (1996) 1751.
[6] E. Kukk, A. Lymboussaki, S. Taira, A. Kaipainen, M. Jeltsch, V. Joukov, K. Alitalo, VEGF-C receptor binding and pattern of expression with VEGFR-3 suggests a role in lymphatic vascular development, Development 122(12) (1996) 3829-37.
[7] A. Lymboussaki, B. Olofsson, U. Eriksson, K. Alitalo, Vascular endothelial growth factor (VEGF) and VEGF-C show overlapping binding sites in embryonic endothelia and distinct sites in differentiated adult endothelia, Circ Res 85(11) (1999) 992-9.
[8] M.J. Karkkainen, A. Saaristo, L. Jussila, K.A. Karila, E.C. Lawrence, K. Pajusola, H. Bueler, A. Eichmann, R. Kauppinen, M.I. Kettunen, S. Yla-Herttuala, D.N. Finegold, R.E. Ferrell, K. Alitalo, A model for gene therapy of human hereditary lymphedema, Proc Natl Acad Sci U S A 98(22) (2001) 12677-82.
[9] Y. Xu, L. Yuan, J. Mak, L. Pardanaud, M. Caunt, I. Kasman, B. Larrivee, R. Del Toro, S. Suchting, A. Medvinsky, J. Silva, J. Yang, J.L. Thomas, A.W. Koch, K. Alitalo, A. Eichmann, A. Bagri, Neuropilin-2 mediates VEGF-C-induced lymphatic sprouting together with VEGFR3, J Cell Biol 188(1) (2010) 115-30.
[10] M.J. Karkkainen, P. Haiko, K. Sainio, J. Partanen, J. Taipale, T.V. Petrova, M. Jeltsch, D.G. Jackson, M. Talikka, H. Rauvala, C. Betsholtz, K. Alitalo, Vascular endothelial growth factor C is

required for sprouting of the first lymphatic vessels from embryonic veins, Nat Immunol 5(1) (2004) 74-80.
[11] M. Jeltsch, A. Kaipainen, V. Joukov, X. Meng, M. Lakso, H. Rauvala, M. Swartz, D. Fukumura, R.K. Jain, K. Alitalo, Hyperplasia of lymphatic vessels in VEGF-C transgenic mice, Science 276(5317) (1997) 1423-5.
[12] A. Saaristo, M.J. Karkkainen, K. Alitalo, Insights into the molecular pathogenesis and targeted treatment of lymphedema, Ann N Y Acad Sci 979 (2002) 94-110.
[13] S.A. Stacker, M.G. Achen, L. Jussila, M.E. Baldwin, K. Alitalo, Lymphangiogenesis and cancer metastasis, Nat Rev Cancer 2(8) (2002) 573-83.
[14] L.M. Ellis, The role of neuropilins in cancer, Mol Cancer Ther 5(5) (2006) 1099-107.
[15] M. Caunt, J. Mak, W.C. Liang, S. Stawicki, Q. Pan, R.K. Tong, J. Kowalski, C. Ho, H.B. Reslan, J. Ross, L. Berry, I. Kasman, C. Zlot, Z. Cheng, J. Le Couter, E.H. Filvaroff, G. Plowman, F. Peale, D. French, R. Carano, A.W. Koch, Y. Wu, R.J. Watts, M. Tessier-Lavigne, A. Bagri, Blocking neuropilin-2 function inhibits tumor cell metastasis, Cancer Cell 13(4) (2008) 331-42.
[16] M. Lohela, M. Bry, T. Tammela, K. Alitalo, VEGFs and receptors involved in angiogenesis versus lymphangiogenesis, Curr Opin Cell Biol 21(2) (2009) 154-65.
[17] L. Yuan, D. Moyon, L. Pardanaud, C. Breant, M.J. Karkkainen, K. Alitalo, A. Eichmann, Abnormal lymphatic vessel development in neuropilin 2 mutant mice, Development 129(20) (2002) 4797-806.
[18] B. Favier, A. Alam, P. Barron, J. Bonnin, P. Laboudie, P. Fons, M. Mandron, J.P. Herault, G. Neufeld, P. Savi, J.M. Herbert, F. Bono, Neuropilin-2 interacts with VEGFR-2 and VEGFR-3 and promotes human endothelial cell survival and migration, Blood 108(4) (2006) 1243-50.
[19] A. Starzec, R. Vassy, A. Martin, M. Lecouvey, M. Di Benedetto, M. Crepin, G.Y. Perret, Antiangiogenic and antitumor activities of peptide inhibiting the vascular endothelial growth factor binding to neuropilin-1, Life Sci 79(25) (2006) 2370-81.
[20] T. Teesalu, K.N. Sugahara, V.R. Kotamraju, E. Ruoslahti, C-end rule peptides mediate neuropilin-1-dependent cell, vascular, and tissue penetration, Proc Natl Acad Sci U S A 106(38) (2009) 16157-62.
[21] A. Jarvis, C.K. Allerston, H. Jia, B. Herzog, A. Garza-Garcia, N. Winfield, K. Ellard, R. Aqil, R. Lynch, C. Chapman, B. Hartzoulakis, J. Nally, M. Stewart, L. Cheng, M. Menon, M. Tickner, S. Djordjevic, P.C. Driscoll, I. Zachary, D.L. Selwood, Small molecule inhibitors of the neuropilin-1 vascular endothelial growth factor A (VEGF-A) interaction, J Med Chem 53(5) (2010) 2215-26.
[22] M.W. Parker, A.D. Linkugel, C.W. Vander Kooi, Effect of C-Terminal Sequence on Competitive Semaphorin Binding to Neuropilin-1, J Mol Biol (2013).
[23] H.F. Guo, X. Li, M.W. Parker, J. Waltenberger, P.M. Becker, C.W. Vander Kooi, Mechanistic Basis for the Potent Anti-Angiogenic Activity of Semaphorin 3F, Biochemistry (2013).
[24] W.C. Darbonne, X. Du, P. Dhawan, D. Hartley, J. Tarrant, H. Taylor, G. Cain, L.M. Shih, R.K. Brachmann, Q. Phung, C.D. Weekes, P. LoRusso, A. Patnaik, H. Xiang, V. Ramakrishnan, Mechanism for platelet reduction in anti-neuropilin-1 (MNRP1685A)–treated phase I patients. , J Clin Oncol 29 (2011) e13598.
[25] W.Q. Liu, Y. Lepelletier, M. Montes, L. Borriello, R. Jarray, R. Grepin, B. Leforban, A. Loukaci, R. Benhida, O. Hermine, S. Dufour, G. Pages, C. Garbay, F. Raynaud, R. Hadj-Slimane, L. Demange, NRPa-308, a new neuropilin-1 antagonist, exerts in vitro anti-angiogenic and anti-proliferative effects and in vivo anti-cancer effects in a mouse xenograft model, Cancer Lett 414 (2017) 88-98.

[26] A.V. Timoshenko, S. Rastogi, P.K. Lala, Migration-promoting role of VEGF-C and VEGF-C binding receptors in human breast cancer cells, Br J Cancer 97(8) (2007) 1090-8.
[27] M.J. Stanton, S. Dutta, H. Zhang, N.S. Polavaram, A.A. Leontovich, P. Honscheid, F.A. Sinicrope, D.J. Tindall, M.H. Muders, K. Datta, Autophagy control by VEGF-C/NRP-2 axis in cancer and its implication for treatment resistance, Cancer Res (2012).
[28] H.L. Goel, B. Pursell, C. Chang, L.M. Shaw, J. Mao, K. Simin, P. Kumar, C.W. Vander Kooi, L.D. Shultz, D.L. Greiner, J.H. Norum, R. Toftgard, C. Kuperwasser, A.M. Mercurio, GLI1 regulates a novel neuropilin-2/alpha6beta1 integrin based autocrine pathway that contributes to breast cancer initiation, EMBO Mol Med 5(4) (2013) 488-508.
[29] M.H. Muders, H. Zhang, E. Wang, D.J. Tindall, K. Datta, Vascular endothelial growth factor-C protects prostate cancer cells from oxidative stress by the activation of mammalian target of rapamycin complex-2 and AKT-1, Cancer Res 69(15) (2009) 6042-8.
[30] C.W. Vander Kooi, M.A. Jusino, B. Perman, D.B. Neau, H.D. Bellamy, D.J. Leahy, Structural basis for ligand and heparin binding to neuropilin B domains, Proc Natl Acad Sci U S A 104(15) (2007) 6152-7.
[31] M.W. Parker, L.M. Hellman, P. Xu, M.G. Fried, C.W. Vander Kooi, Furin processing of semaphorin 3F determines its anti-angiogenic activity by regulating direct binding and competition for neuropilin, Biochemistry 49(19) (2010) 4068-75.
[32] M.W. Parker, P. Xu, X. Li, C.W. Vander Kooi, Structural basis for selective vascular endothelial growth factor-A (VEGF-A) binding to neuropilin-1, J Biol Chem 287(14) (2012) 11082-9.
[33] M.W. Parker, A.D. Linkugel, H.L. Goel, T. Wu, A.M. Mercurio, C.W. Vander¬†Kooi, Structural Basis for VEGF-C Binding to Neuropilin-2 and Sequestration by a Soluble Splice Form, Structure 23(4) (2015) 677-687.
[34] L. Muley, B. Baum, M. Smolinski, M. Freindorf, A. Heine, G. Klebe, D.G. Hangauer, Enhancement of hydrophobic interactions and hydrogen bond strength by cooperativity: synthesis, modeling, and molecular dynamics simulations of a congeneric series of thrombin inhibitors, J Med Chem 53(5) (2010) 2126-35.
[35] A.M. Said, D.G. Hangauer, Binding cooperativity between a ligand carbonyl group and a hydrophobic side chain can be enhanced by additional H-bonds in a distance dependent manner: A case study with thrombin inhibitors, Eur J Med Chem 96 (2015) 405-24.
[36] A.M. Said, D.G. Hangauer, Ligand binding cooperativity: Bioisosteric replacement of CO with SO2 among thrombin inhibitors, Bioorg Med Chem Lett 26(16) (2016) 3850-4.
[37] M.W. Parker, P. Xu, H.F. Guo, C.W. Vander Kooi, Mechanism of Selective VEGF-A Binding by Neuropilin-1 Reveals a Basis for Specific Ligand Inhibition, PLoS One 7(11) (2012).
[38] A. Starzec, P. Ladam, R. Vassy, S. Badache, N. Bouchemal, A. Navaza, C.H. du Penhoat, G.Y. Perret, Structure-function analysis of the antiangiogenic ATWLPPR peptide inhibiting VEGF(165) binding to neuropilin-1 and molecular dynamics simulations of the ATWLPPR/neuropilin-1 complex, Peptides 28(12) (2007) 2397-402.
[39] M.A. von Wronski, N. Raju, R. Pillai, N.J. Bogdan, E.R. Marinelli, P. Nanjappan, K. Ramalingam, T. Arunachalam, S. Eaton, K.E. Linder, F. Yan, S. Pochon, M.F. Tweedle, A.D. Nunn, Tuftsin binds neuropilin-1 through a sequence similar to that encoded by exon 8 of vascular endothelial growth factor, J Biol Chem 281(9) (2006) 5702-10.
[40] W.Q. Liu, Y. Lepelletier, M. Montes, L. Borriello, R. Jarray, R. Grepin, B. Leforban, A. Loukaci, R. Benhida, O. Hermine, S. Dufour, G. Pages, C. Garbay, F. Raynaud, R. Hadj-Slimane, L. Demange, NRPa-308, a new neuropilin-1 antagonist, exerts in vitro anti-angiogenic and anti-

proliferative effects and in vivo anti-cancer effects in a mouse xenograft model, Cancer Lett 414 (2018) 88-98.
[41] J. Powell, F. Mota, D. Steadman, C. Soudy, J.T. Miyauchi, S. Crosby, A. Jarvis, T. Reisinger, N. Winfield, G. Evans, A. Finniear, T. Yelland, Y.T. Chou, A.W.E. Chan, A. O'Leary, L. Cheng, D. Liu, C. Fotinou, C. Milagre, J.F. Martin, H. Jia, P. Frankel, S. Djordjevic, S.E. Tsirka, I.C. Zachary, D.L. Selwood, Small Molecule Neuropilin-1 Antagonists Combine Antiangiogenic and Antitumor Activity with Immune Modulation through Reduction of Transforming Growth Factor Beta (TGFbeta) Production in Regulatory T-Cells, J Med Chem 61(9) (2018) 4135-4154.
[42] D. Tymecka, A.K. Puszko, P.F.J. Lipinski, B. Fedorczyk, B. Wilenska, K. Sura, G.Y. Perret, A. Misicka, Branched pentapeptides as potent inhibitors of the vascular endothelial growth factor 165 binding to Neuropilin-1: Design, synthesis and biological activity, Eur J Med Chem 158 (2018) 453-462.
[43] M.W. Parker, C.W. Vander Kooi, Microplate-based screening for small molecule inhibitors of neuropilin-2/vascular endothelial growth factor-C interactions, Anal Biochem 453 (2014) 4-6.
[44] M.W. Parker, A.D. Linkugel, C.W. Vander Kooi, Effect of C-terminal sequence on competitive semaphorin binding to neuropilin-1, J Mol Biol 425(22) (2013) 4405-14.
[45] B.A. Jardin, Y. Zhao, M. Selvaraj, J. Montes, R. Tran, S. Prakash, C.B. Elias, Expression of SEAP (secreted alkaline phosphatase) by baculovirus mediated transduction of HEK 293 cells in a hollow fiber bioreactor system, J Biotechnol 135(3) (2008) 272-80.
[46] R.A. Laskowski, M.B. Swindells, LigPlot+: multiple ligand-protein interaction diagrams for drug discovery, J Chem Inf Model 51(10) (2011) 2778-86.
[47] K.B. Santos, I.A. Guedes, A.L.M. Karl, L.E. Dardenne, Highly Flexible Ligand Docking: Benchmarking of the DockThor Program on the LEADS-PEP Protein-Peptide Data Set, J Chem Inf Model 60(2) (2020) 667-683.

Highlights:

1. Nrp2 is critically involved in tumor metastasis.
2. There is no known small molecule inhibitor specific for Nrp2.
3. Identified a benzamidine based small molecule inhibitor with Nrp2 selectivity.
4. SAR was utilized to optimize potency and selectivity for Nrp2.

Declaration of interests

☒ The authors declare that they have no known competing financial interests or personal relationships that could have appeared to influence the work reported in this paper.

☐The authors declare the following financial interests/personal relationships which may be considered as potential competing interests: